[1]G. P. Arnold, P. J. Bendt, and E. C. Kerr, Phys. Rev. 113, 1379 (1959).
[2]R. A. Cowley and A. D. B. Woods, Can. J. Phys. 49, 177 (1971).
[3]C. E. Chase, Proc. Roy. Soc. (London) A220, 116 (1953).
[4]The sound speed referred to here is that of "first sound," whereas the theoretical discussion of this paper is concerned with "zero sound." The two speeds are nearly the same (as evidenced by the fact that the first-sound speed is a good approximation to the limiting low-k slope of the excitation spectrum), and so the distinction does not affect the argument presented here.
[5]K. R. Atkins and R. A. Stasior, Can. J. Phys. 31, 1156 (1953).
[6]N. N. Bogoliubov, J. Phys. USSR 11, 7 (1942) (reprinted in Ref. 21).
[7]S. T. Beliaev, Zh. Eksperim. i Teor. Fiz. 34, 443 (1959) [Sov. Phys. JETP 7, 299 (1958)].
[8]N. Shohno, Progr. Theoret. Phys. (Kyoto) 31, 553 (1964); 32, 370 (1964); M. Luban and W. D. Grobman, Phys. Rev. Letters 17, 182 (1966); D. H. Kobe, Ann. Phys. (N.Y.) 47, 15 (1968).
[9]M. Luban, Phys. Rev. 128, 965, (1962).
[10]M. Girardeau and R. Arnowitt, Phys. Rev. 113, 755 (1959).
[11]Iu. A. Tserkovnikov, Dok. Akad. Nauk (SSSR) 120, 991 (1958) [Sov. Phys. Doklady 3, 603 (1958)].
[12]Other related peculiarities of these models are discussed by L. Reatto and J. P. Straley, Phys. Rev. 183, 321 (1970).
[13]L. D. Landau, J. Phys. USSR 5, 71 (1941); 11, 91 (1947) [reprinted in I. M. Khalatnikov, *Introduction to the Theory of Superfluidity* (Benjamin, New York, 1965), pp. 185, 205].
[14]P. J. Bendt, R. D. Cowan, and J. L. Yarnell, Phys. Rev. 113, 1386 (1959).
[15]J. Gavoret and P. Nozieres, Ann. Phys. (N.Y.) 28, 349 (1964).
[16]K. Huang and A. Klein, Ann. Phys. (N.Y.) 30, 203 (1964).
[17]P. Hohenberg and P. C. Martin, Ann. Phys. (N.Y.) 34, 346 (1965).
[18]L. P. Kadanoff and G. Baym, *Quantum Statistical Mechanics* (Benjamin, New York, 1962), p. 14.
[19]N. M. Hugenholtz and D. Pines, Phys. Rev. 116, 489 (1959).
[20]T. H. Cheung and A. Griffin, Can. J. Phys. 48, 2135 (1970).
[21]D. Pines, *The Many Body Problem* (Benjamin, New York, 1962), p. 46.
[22]J. Goldstone and K. Gottfried, Nuovo Cimento 13, 849 (1959).
[23]R. D. Etters, Phys. Rev. Letters 16, 119 (1966).
[24]J. Bardeen, L. Cooper, and J. Schrieffer, Phys. Rev. 108, 1175 (1957).

PHYSICAL REVIEW A VOLUME 5, NUMBER 1 JANUARY 1972

Experimental Investigation of Transient Stimulated Raman Scattering in a Linearly Dispersionless Medium

R. L. Carman*†
Harvard University, Gordon McKay Laboratory, Cambridge, Massachusetts 02138
and
M. E. Mack‡
United Aircraft Research Laboratories, East Hartford, Connecticut 06108
(Received 5 May 1971)

The results of numerical calculations of the transient stimulated Raman scattering reported previously have been verified experimentally under conditions where both linear dispersion and self-focusing effects were negligible. The existence of a delay between maxima of the laser and Stokes pulses is experimentally demonstrated for the first time, while the pulse shortening in time via Raman scattering is established more firmly than in previous work. The incident-laser-pulse duration, generated-Stokes-pulse duration, and delay between intensity maxima for the laser and Stokes pulses were measured with the two-photon absorption-fluorescence technique. The effective phonon-dephasing time is determined via spontaneous Raman scattering. By using these measured quantities, inferences are made as to the magnitude of the transient gain and the shape of the exciting picosecond laser pulse.

I. INTRODUCTION

Stimulated Raman scattering (SRS) induced by picosecond-duration light pulses has been discussed by many authors from both an experimental[1] and theoretical[2,3] point of view. Realistic numerical calculations in this transient regime recently performed took into account practical laser-pulse shapes in predicting the Stokes-pulse duration, the SRS gain, and the delay between the peak amplitudes of the Stokes and laser light pulses.[3] Earlier experimental work suggested that in the case of picosecond-duration light pulses generated by a mode-locked ruby laser, the Stokes pulses were

certainly no longer in duration than the pump pulses.[4] Three serious limitations to this earlier work were the presence of strong self-focusing in the CCl_4, the lack of control in the gain leading to a high probability of saturation and laser depletion, and the presence of significant linear dispersion, the deleterious effects of which were indicated in previous work.[3]

In this paper, we will present data on a system with negligible dispersion which verify many features of the numerical results under conditions where self-focusing and laser depletion can be neglected. In addition, the data add further support to the notion that the pulse should have a time distribution which is close to Gaussian.[5] In Sec. II, the method of selection of the sample medium is discussed. The discussion includes estimates of the transient vibrational SRS gain coefficient, of the effects of rotational SRS, and of the amount of linear dispersion between the laser and Stokes frequencies, all of which are important factors in the evaluation of possible sample gases. Checks for the unimportance of self-focusing under the required operating conditions are also discussed. Sec. III is devoted to the experimental technique and the presentation and discussion of data. Section IV summarizes the significance of this work and indicates some future extensions.

II. SAMPLE SELECTION

Of vital importance to a carful study of transient SRS is the absence of the effects of both linear dispersion and self-focusing. As a result, much effort was expended in selecting a material which would minimize both. Linear dispersion tends to cause the Stokes wave packet to either speed ahead (normal dispersion) or lag behind (anomalous dispersion) the laser wave packet. Since the transiency introduces a delay of the Stokes-amplitude peak with respect to the laser-amplitude peak, dispersion will either improve or degrade the synchronism of the two wave packets, or, more importantly, of their phases. The net result is an alteration of the parameters associated with the Stokes pulse, including the magnitude and dependence of the gain coefficient. The criterion for determining the importance of dispersion was presented in earlier work.[3] For dispersive effects to be negligible, the phase synchronism length determined by dispersion must be much greater than the length required for the gain to restore the constant phase difference between the laser and Stokes field. This is the case if

$$\frac{\pi}{[(\partial k/\partial\omega)_L - (\partial k/\partial\omega)_s]\, c\Delta\bar{\nu}} \gg \frac{2\Delta\bar{\nu}}{g_{ss}\Gamma} \quad , \tag{1}$$

where $\Delta\bar{\nu}$ is the laser pump linewidth in the medium, $e^{g_{ss}z}$ is the steady-state SRS gain for the same intensity, and Γ is the molecular vibrational linewidth, all expressed in units of cm^{-1}. Thus, the quantity to be minimized is

$$(\Delta\bar{\nu})^2\, c\left|\left(\frac{\partial k}{\partial\omega}\right)_L - \left(\frac{\partial k}{\partial\omega}\right)_s\right| \quad .$$

It is clear from Eq. (1) that it is unwise to use a laser the bandwidth of which is much larger than is required to cause a transient response if dispersive effects are to be made small. At this point, it is convenient to define the ratio of the velocity of light in vacuum and the group velocity of the wave packet in the medium n_g, which is basically the analog of the index of refraction n in the case of the phase velocity, or

$$n_g \equiv c\frac{\partial k}{\partial\omega} = n - \lambda\frac{\partial n}{\partial\lambda} \quad , \tag{2}$$

where λ is the wavelength of the light in vacuum. Restating Eq. (1), in terms of the group index difference $\Delta n_g = |(n_g)_L - (n_g)_s|$, we find

$$\Delta n_g \ll \pi g_{ss}\Gamma/2(\Delta k)^2 \quad . \tag{3}$$

In Table I, both n and n_g are given for the number of gases at atmospheric pressure and 0 °C. For purposes of comparison, a few liquids are also included. The values of Δn_g indicated for the gases are those obtained by scaling up linearly to the typical operating pressure at which vibrational SRS would be observed. When the operating pressure is close to the liquification pressure at room temperature, one should scale with the density, as was done for SF_6 in Table I, instead of with pressure. In the other materials operated close to liquification, Δn_g in Table I is too low by the ratio $\rho_{op}/(\rho_{1atm}\, P)$. Even at the very high required pressure, gases are more than an order of magnitude less dispersive than are liquids.

The gases listed in Table I represent relatively high Raman-gain materials which are available at reasonably high pressure and whose stimulated Raman shifted components have been observed.[6] In addition to the vibrational SRS component, the rotational analog has also been observed with picosecond pulse excitation[6] for the cases of N_2O, CO_2, and O_2. In Table II, estimates of the transient vibrational SRS gain and the rotational Raman γ^2 are given, where γ is the anisotropic part of the molecular-polarizability tensor. The rotational SRS cross section is proportional to γ^2. It is clear from Table II that both ethylene and chlorine gas should also have stimulated rotational Raman bands. The existence of rotational SRS is important because it represents a competing mode of operation and because it effectively increases the line width $\Delta\bar{\nu}$ of the pump causing dispersion to be more important for the vibrational SRS. Therefore, all

TABLE I. Dispersion data.

Material	Δk	β' [a]	λ_0^{-2} [a]	$\lambda(\mu)$	$10^6(n-1)$	$(10^6)-\lambda\frac{\partial n}{\partial\lambda}$	$10^6(n_g-1)$	P(atm)	$10^6\,\Delta n_g$
				Gases					
SF_6	775 cm^{-1}	211 400[b]	279.39[b]	0.6943	762.3	11.4	773.7	18	
				0.7338	761.7	10.2	771.9		50[c]
N_2	2330 cm^{-1}	55 939	187.94	0.6943	297.8	6.6	304.4	100	
				0.8284	296.8	4.6	301.4		300
NH_3	3339 cm^{-1}	32 953	90.392	0.6943	373.1	17.5	390.6	86	
				0.9035	369.6	10.2	379.8		93[d]
NO	1877 cm^{-1}	39 122	135.73	0.6943	292.7	9.1	301.8	34	
				0.7984	291.6	6.8	298.4		120
N_2O	1285 cm^{-1}	62 983	126.84	0.6943	504.8	16.8	521.6	50	
				0.7624	503.4	13.8	517.2		220[d]
O_2	1555 cm^{-1}	37 744	142.27	0.6943	269.2	8.0	277.2	100	
				0.7784	268.4	6.3	274.7		250
CO_2	1388 cm^{-1}	69 049	156.63	0.6943	446.8	12.0	458.8	58	
				0.7684	445.7	9.7	455.4		200[d]
CO	2145 cm^{-1}	40 452	123.60	0.6943	332.9	11.4	344.3	100	
				0.8157	331.3	8.2	339.5		480
CH_4	2914 cm^{-1}	55 739[b]	129.15[b]	0.6943	438.6	14.3	452.9	100	
				0.8705	436.1	9.0	445.1		780
C_2H_4	1342 cm^{-1}	59 995[b]	86.704[b]	0.6943	708.9	34.8	743.7	55	
				0.7657	705.9	28.4	734.3		520[d]
C_3H_6	2924 cm^{-1}	96 798[b]	94.925[b]	0.6943	1042.5	46.6	1089.1	9	
				0.8712	1034.1	29.1	1063.2		233
H_2	4160 cm^{-1}	18 800	137.88	0.6943	138.4	4.2	142.6	100	
				0.9763	137.4	2.1	137.5		510
HCl	2886 cm^{-1}	51 583	118.49	0.6943	433.1	15.8	458.9	42	
				0.8683	440.3	10.0	450.3		360[d]
HBr	2558 cm^{-1}	57 162	96.316	0.6943	606.6	26.7	633.3	22	
				0.8941	601.3	15.8	617.1		360[d]
Cl_2	556 cm^{-1}	81 257	106.993	0.6943	774.5	30.6	805.1	6.6	24[d]
				0.7222	773.3	28.2	801.5		

Material	Δk	a[e]	b[e]	λ_0^2[e]	d[e]	$\lambda(\mu)$	n	$-\lambda\frac{\partial n}{\partial\lambda}$	n_g	$(10^6)\Delta n_g$
					Liquids					
CS_2	656 cm^{-1}	2.515 16	0.041 695	0.047 319 3	0.000 3	0.6943	1.615 84	0.065 91	1.681 75	
(T = 18 °C)						0.7274	1.612 93	0.059 02	1.671 95	9 800
C_6H_6	991 cm^{-1}	2.194	0.024 09	0.017 14		0.6943	1.498 60	0.035 85	1.534 45	
(T = 20 °C)						0.7456	1.496 23	0.030 83	1.527 06	7 400
	3064 cm^{-1}					0.8819	1.491 87	0.021 71	1.513 58	21 000
H_2O	3651 cm^{-1}	1.761 48	0.006 543 8	0.013 252 61	0.013 414	0.6943	1.330 03	0.015 65	1.345 68	
(T = 20 °C)						0.9301	1.325 73	0.014 64	1.340 37	5 300

[a] $(n-1)^{0\,°C}_{760} = 10^{-5}\beta'/(\lambda_0^{-2}-\lambda^{-2})$; values taken from *International Critical Table I* (McGraw-Hill, New York, 1930), p. 11.
[b] Calculated from data in Landolt-Börnstein, *Zahlerwerte und Funktionen aus Physik, Chemi, Astromie, Geophysik, und Technik* (Springer, Berlin, 1957), Vol. 6, p. 881.
[c] Known density change from 1 atm to P was used to linearly extrapolate.
[d] Owing to P being close to the liquification point, linear extrapolation yields this lower limit.
[e] $n^2 = a + b/(\lambda^2-\lambda_0^2) - \lambda^2 d$; values taken from Ref. a, pp. 12–16.

five of the gases N_2O, CO_2, O_2, Cl_2, and C_2H_4 must be eliminated as sample candidates.

Of the remaining ten gases in Table I, SF_6 is the least dispersive by a factor between 2 and 45. Although values of $\partial\alpha/\partial R$ and R are not available for SF_6, the very low threshold for transient vibra-

TABLE II. Raman-gain data.

Gas	Vibrational							Rotational		
	$(\nu/c)_{vib}$	$(\nu/c)_{Stokes}$	$\rho^{0\,°C}_{1\,atm}$ [a]	$\left(\frac{\partial\alpha}{\partial R}\right)_{exp}$ [b]	$G_T^{vib}/(PW_Lz)^{1/2}$ [c]	$G_T^{vib}/(W_Lz)^{1/2}$ [c]	R [d]	$\alpha_0^{0\,°C}$	γ [e]	γ^2
	(cm^{-1})	(cm^{-1})	(g/l)	(10^{-16} cm^2)	(atm J/cm)$^{-1/2}$	(J/cm)$^{-1/2}$	(depol. ratio)	(10^{-24} cm^3)	(10^{-24} cm^3)	(10^{-48} cm^6)
SF_6	775	13 625	6.602					4.58		
N_2	2330	12 072	1.250 5	1.69	1.67×10^{-2}	1.67×10^{-1}	0.036	1.80	1.36	1.85
NH_3	334	11 066	0.771 40	1.00	1.01×10^{-2}	0.30×10^{-1} [f]	0.011	2.21	0.90	0.81
NO	1877	12 525	1.230 2					1.73		
N_2O	1285	13 117	1.977 5				0.125	2.99	4.49	20.16
O_2	1555	12 845	1.428 96	1.43	1.67×10^{-2}	1.67×10^{-1}	0.065	1.59	1.64	2.69
CO_2	1388	13 012	1.976 93	1.83	1.94×10^{-2}	1.48×10^{-1} [f]	0.097	2.65	3.43	11.76
CO	2145	12 255	1.250 0	1.44	1.50×10^{-2}	1.50×10^{-1}	0.015	1.97	1.04	1.08
CH_4	2914	11 486	0.716 82	1.04	1.19×10^{-2}	1.19×10^{-1}	0.013	2.60	1.16	1.35
C_2H_4	1342	13 060	1.260 46				0.029	4.20	2.83	8.01
C_3H_6	2924	11 478	1.914 9					6.17		
H_2	4160	10 242	0.089 88				0.026	0.820	0.599	0.269
HCl	2886	11 514	1.639 11	1.00	0.76×10^{-2}	0.45×10^{-1} [f]	0.007	2.62	0.850	0.723
HBr	2558	11 842	3.644 2	1.20	0.67×10^{-2}	0.30×10^{-1} [f]				
Cl_2	556	13 846	3.214				0.042	4.59	3.75	14.06

[a] ρ = density obtained from *Handbook of Chemistry and Physics* (Chemical Rubber Publishing Co., Cleveland, 1964).

[b] E. R. Lippincott and G. Nagarajan, Bull. Soc. Chim. Belges 74, 551 (1965).

[c] $(g_T)^{vib} = [(W_Lz)32\pi^2N^2(\nu/c)_{Stokes}(\partial\alpha/\partial\gamma)^2P/\rho^{0\,°C}_{1\,atm}(\nu/c)_{vib}c^2\epsilon_0]^{1/2}$, where W_L is the laser intensity, P is the pressure in atomspheres and $\partial\alpha/\partial\gamma$ is the Raman polarizability derivative.

[d] G. Placzek, *Handbuch der Radiologie*, edited by Erich Marx (Akademische Zerlagsgesellschaft, Leipzig, 1934), p. 209-374 (URCL Transl. No. 526).

[e] $\gamma \cong \alpha_0[45R/3-4R]^{1/2}$, where $\alpha_0 \cong n - 1/2\pi N$.

[f] As in Table I (near liquification pressures) the scaling should be with density from standard conditions, not with pressure. Therefore, these numbers are approximate.

tional SRS as well as the very high conversion efficiencies (up to 70%) observed experimentally[6] indicate a large vibrational Raman cross section. In addition, we have never observed rotational SRS in SF_6 under any conditions.

The remaining question of the importance of self-focusing effects at our required operating conditions was then investigated for SF_6. A mode-locked ruby laser was used which produced approximately 10–15 mJ per pulse within a 0.5×1.0 cm elliptical cross section at a divergence angle of between 0.5 and 1 mrad.[7] The output intensity profile was locally uniform over at least 2 mm. Near-field photographs of the collimated beam passing through a 50-cm cell were indistinguishable with and without gas. Also, investigations were made of both the laser and Stokes beam spatial profile in the case of focusing the pump with a 50-cm lens.[8] Again no spatial effects were attributable to self-focusing. Finally, using the measured self-focusing threshold in liquid SF_6,[9] and extrapolating to gas density indicates that much higher field strengths would be required for self-focusing to be important than are needed for SRS.

III. EXPERIMENTAL RESULTS

The experiments were performed with the mode-locked ruby laser described in Sec. II at output energies of between 5 and 10 mJ per pulse. The beam was focused with a 1-m focal length lens into the 50-cm-long cell of SF_6. The SF_6 operating pressure was 18 atm. The diagnostics are illustrated in Fig. 1. Both incident and transmitted laser energies per pulse were monitored by photodiode 1, and data were taken only when both signals were the same height to within 5% for each pulse. At such a low conversion efficiency, over-all laser depletion is not important. In the absence of self-focusing local laser depletion effects are avoided as well. A second fast-risetime photodiode (2) monitored the Stokes energy generated per pulse. Figure 2 shows corresponding laser and Stokes pulse trains under strong conversion conditions. Typical laser depletion oscillograms are shown in Figs. 3(a) and 3(b) under acceptable conditions. Figure 3(c) shows the result of either raising the laser output or changing to a 50-cm focal length lens at the cell input.

The two-photon absorption fluorescence setup, illustrated in Fig. 1, was isolated from the experiment by Filter 3, which had a factor of 100 attenuation per pass at the laser frequency. Filter 3 also had the property of making the laser and Stokes intensities comparable under the operating conditions described above. A cylindrical lens was used to intensify the overlap region and had the additional advantage of reducing the depth of field requirements of the camera lens. Filters 5 and 6 were of equal optical path length, and were used in the following three modes in conjunction with Filter 4: (1) Filters 5 and 6 were removed completely and Filter

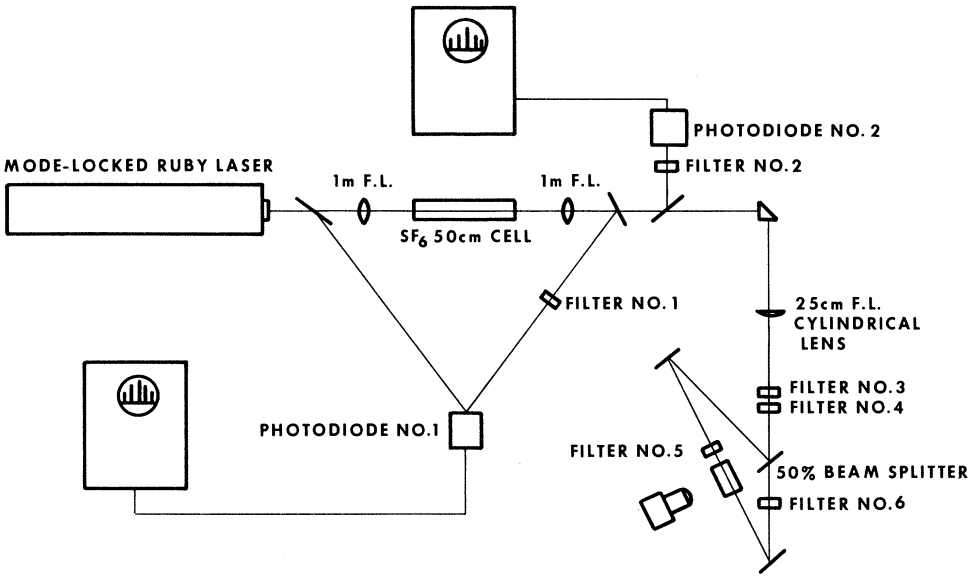

FIG. 1. Illustration of experimental setup.

4 was an ir cutoff filter transmitting just the laser beam. This resulted in a laser pulse duration measurement. (2) Filters 5 and 6 were removed completely and Filter 4 was a uv cutoff filter transmitting just the Stokes beam. This resulted in a Stokes-pulse duration measurement. (3) Filter 4 was absent, and Filter 5 was a uv cutoff filter while Filter 6 was an ir cutoff filter. This resulted in running the forward directed laser beam against the beam-split Stokes beam. This display should have been undisplaced from that of conditions (1) and (2) if no delay existed and the pulse duration measured in (3) should be that of the longer pulse duration. For good contrast in the two photon absorption-fluorescence photographs, the Stokes and laser intensities in the overlap region must be nearly equal. Because we require operation, which avoids saturation and laser depletion, small fluctuations in the laser output intensity results in large variations in the relative Raman cell output beam intensities. As a result a large number of laser firings were required to obtain useable data.

In order to avoid errors due to a systematic change in the operation of the laser, data were taken in cycles, where each cycle involved going through the above modes sequentially. Using about 2.5-psec-duration laser pulses, the Stokes duration t_s was consistently about a third shorter than the laser duration t_L. This is in contrast to the CCl_4 work,[4] where $t_s > t_L$ as well as $t_s < t_L$ was encountered. A typical output display for the 2.5-psec-duration excitation is shown in Fig. 4.

Using these short pulses, it would be very difficult to determine quantitatively the size of any delay between the laser and Stokes pulse peaks since the delay would be expected to be less than one-laser-pulse duration.[3] Consequently, the laser-pulse duration was lengthened to $\tau_L \approx 15$ psec. The time-bandwidth product remained at unity.[7]

In Fig. 5 we show two traces of the spontaneous Raman linewidth Γ of the 775-cm^{-1} mode in SF_6, which indicate that the response will still be transient with the longer pulses. Trace (a) was taken using a Spex double grating monochromator in conjunction with an argon laser operating on the 5145-Å line. The measured width was 2.75 cm^{-1} for the Stokes plus slit function, while the laser line measured 1.1 cm^{-1} (pure slit function), corresponding

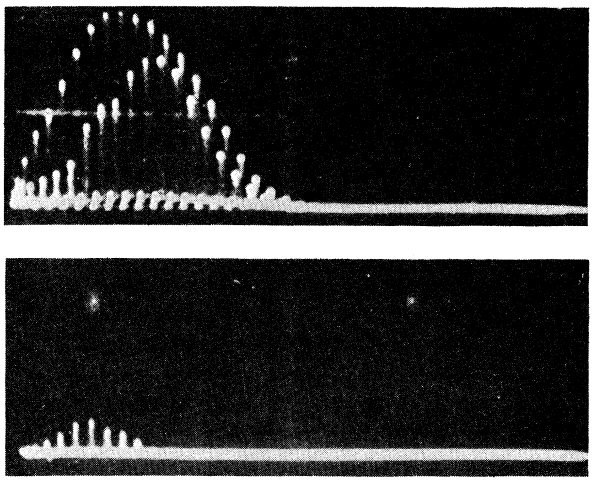

FIG. 2. Oscillograms of pulse trains demonstrating high Raman conversion: (a) interleafed incident and transmitted laser pulses; (b) generated Stokes-pulse train.

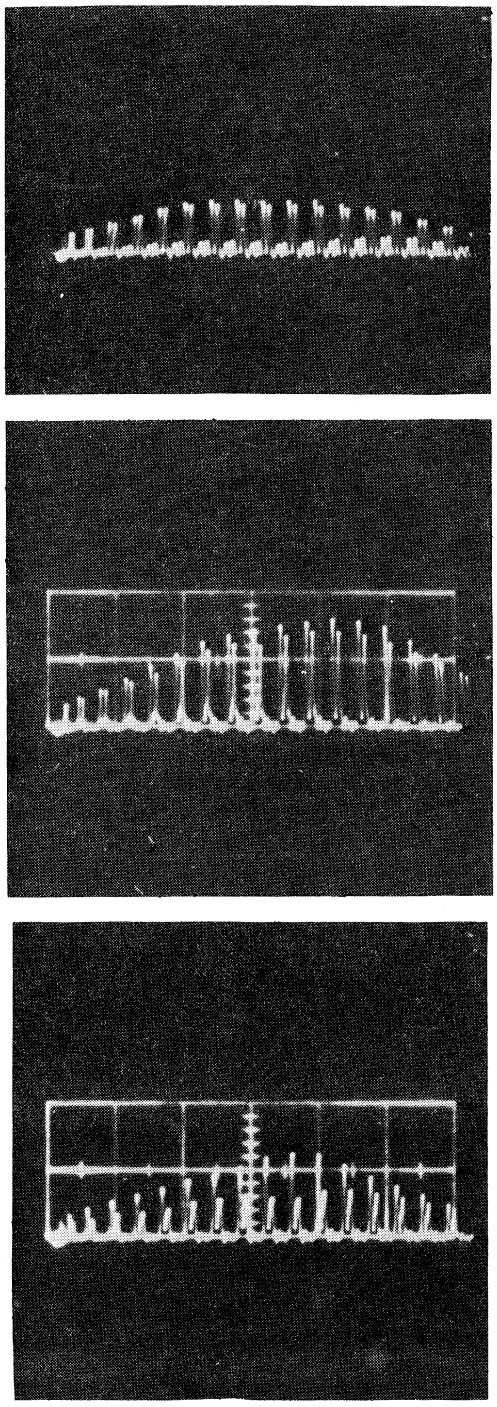

FIG. 3. Oscillograms of interleafed incidence and transmitted laser-pulse trains. (a) Typical oscillogram under conditions where the laser depletion was small enough to be acceptable; (b) marginal laser depletion; (c) example of unacceptably large laser depletion.

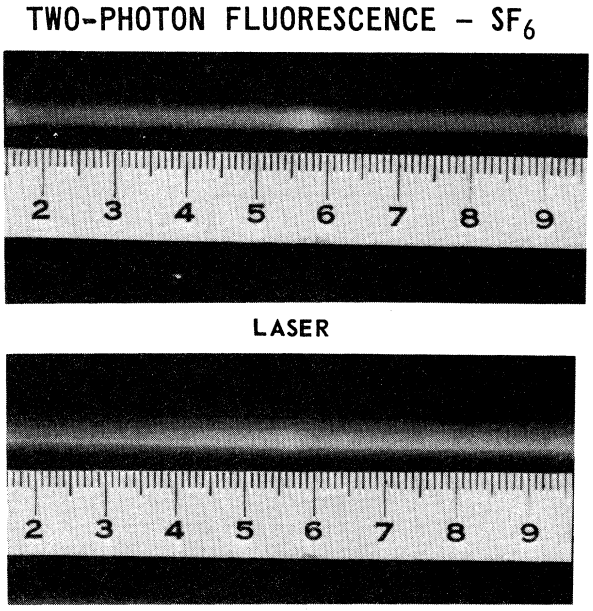

FIG. 4. Example of two-photon absorption fluorescence data under conditions of 2.5-psec-duration excitation, demonstrating shorter duration generated Stokes pulses.

to an actual line width for the SF_6 775-cm^{-1} mode of $\Gamma \cong 1.65$ cm^{-1}. Trace (b) was taken using a piezoelectrically scanned Fabry-Perot interferometer in conjunction with a multichannel analyzer and the same argon laser. While 90-min integration times were required with a 1-sec scan time, the very weak signal was sufficiently large after filtering

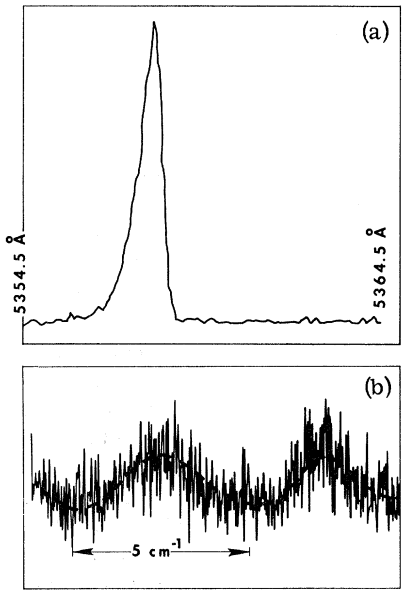

FIG. 5. Spectrograms showing spontaneous Raman linewidths of the 775-cm^{-1} mode in SF_6 taken at 18 atm and with (a) double Spex grating monochrometer, and (b) piezoelectrically scanned Fabry Perot interferometer.

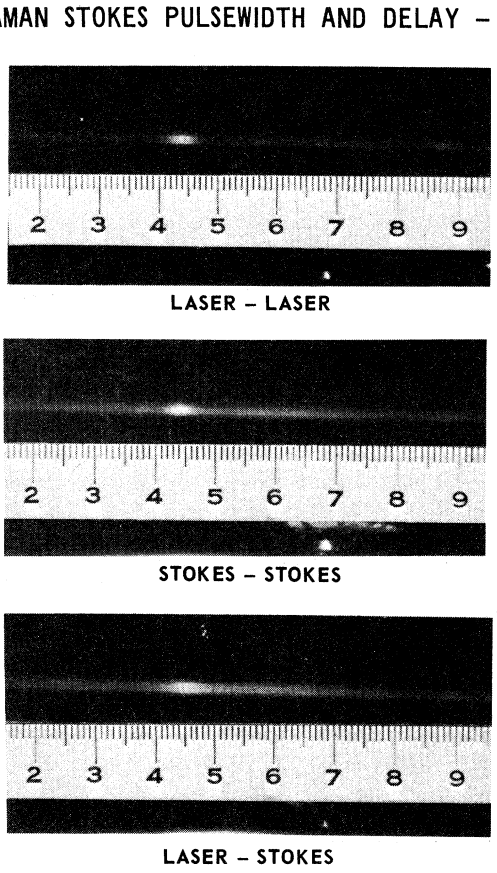

FIG. 6. Typical two-photon absorption fluorescence data taken using approximately a 15-psec-duration laser pulse. Note that the laser Stokes pattern is displaced, demonstrating a delay between the Stokes and Laser intensity maxima.

out the laser line to yield a line width of 1.4 ± 0.2 cm^{-1}. The two methods were in good agreement, and a pulse duration of 15 psec was, therefore, justifiable since the condition for transiency is that $\Gamma \ll G_{ss}\,\Delta\nu$, where $e^{G_{ss}}$ is the steady-state gain assuming the same incident intensity. Since significant conversion requires $G_{ss} > 10$, this relationship is satisfied.

The results of experiments carried out with the 15-psec-duration excitation are shown in Fig. 6. The relevant quantities are for a laser-pulse duration $t_L = 15$ psec, the Stokes-pulse duration $t_s = 9$ psec, and the delay between intensity maxima $t_D = 6$ psec. This represents the first experimental verification of the delay as well as the first clear demonstration of the pulse shortening.

In Fig. 7, we have recalculated some of the numerical results[3] which are relevant to these experiments. An important parameter is the product of Γ and $t_L = 1/\Delta\nu$, and for the 15-psec-duration laser pulses, $\Gamma t_L \approx 1$. The second important piece of information is the laser-pulse shape which is now determined since all other parameters have been measured. Figure 7 is for a Gaussian temporal distribution for the laser, and it shows that for $t_s/t_L = 0.6$, we have a transient gain e^{G_t}, where $G_t \approx 9$. Reading vertically, we then find that $t_D/t_L = 0.42$, which is in good agreement with the experimental value. Finally, the corresponding steady-state gain would be $e^{G_{ss}}$, where $G_{ss} = 25$. There are no adjustable parameters in this calculation.

Since all the two photon absorption fluorescence data were not taken simultaneously, one cannot state with certainly that the ruby-laser pulse shape is Gaussian, However, if the time variation of the laser electric field envelope is assumed to be of the form $E_L \propto e^{-|t/T|^n}$, the multiple-shot data described above indicate that n must be in the range $1.5 < n < 3$, where $n = 2$ is the Gaussian, as seen from Fig. 7. Assumed laser-pulse shapes other than exponential are in very poor agreement with the present results.[3]

IV. DISCUSSION

These experiments confirm enough of the details of the transient SRS theory to provide a reasonable confidence in its validity. However, a lack of linear dispersion is the exception in the historically important Raman-active materials, as well as in long-range atmospheric pressure gas paths. Because of the difficulty of the numerical calculations

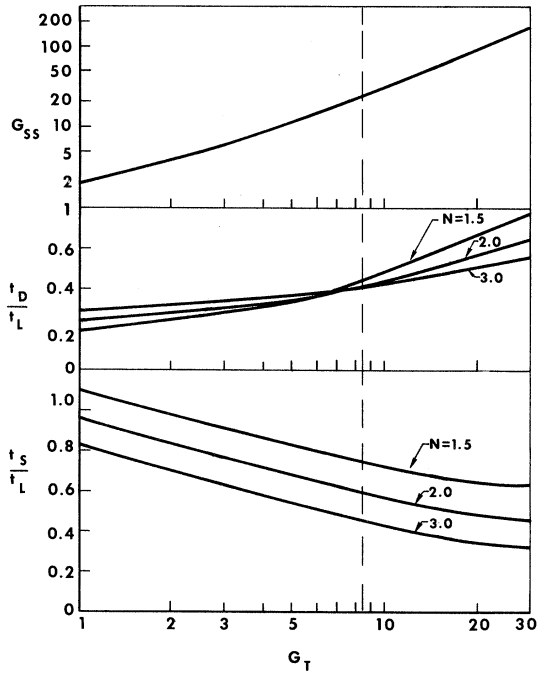

FIG. 7. Calculated parameters for stimulated Raman scattering with $\Gamma t_L = 1$. G_{ss} is the steady-state gain coefficient, t_d the delay, t_s the Stokes-pulse duration, and G_T the transient gain coefficient.

which include linear dispersive effects, experimental confirmation of the present theory under exceptionally clean and simple conditions is very important. These experiments provide that confirmation. In addition, calculations on self-induced transparency and other coherent effects associated with the stimulated Raman process require a complete understanding and description of the low-field effects. Finally, an understanding of the competition between various nonlinear processes such as rotational SRS with vibrational SRS, frequency broadening with SRS, self-focusing with various inelastic stimulated scattering processes, etc., depends on how well we can model the independent processes.

From an experimental point of view, the feasibility of determining approximate laser-pulse shapes using SRS has been demonstrated for the simple case of a pulse of time-bandwidth product unity. In the more complicated cases of the mode-locked Nd: glass laser or mode-locked organic-dye lasers, one may hope to learn something about the reproducibility of any temporal structure, as well as the effective rate of rise and fall of the envelope of any temporal structure. However, the wider-laser-pulse bandwidth and large time-bandwidth product $t_L \Delta\nu$ implies that dispersive effects will play a more important role. In order to do an experiment similar to the one reported here, higher intensities and shorter cell lengths would have to be employed. The condition on the intensity can be obtained directly from Eq. 3, namely,

$$g_{ss} \gg \frac{2(\Delta\bar{\nu})^2 \Delta n_g}{\pi\Gamma} \quad . \tag{3'}$$

Therefore, for the same magnitude of Δn_g and degree of satisfaction of the inequality, the laser intensity must scale quadratically with the bandwidth. This implies that, for the same transient gain, the interaction length z would scale inversely with approximately the laser bandwidth squared times the laser-pulse duration.

---

*Present address: University of California, Lawrence Radiation Laboratory, Livermore, Calif. 94550.

†Work supported by the Joint Services Electronics Program under Contract No. N00014-67-A-0298-0006 and by the National Aeronautics and Space Administration Account No. NGR22-007-117.

‡Work supported by The Advanced Research Projects Agency of the Department of Defense and monitored by The Office of Naval Research under Contract No. N00014-66-C-0344.

[1]S. L. Shapiro, J. A. Giordmaine, and K. W. Wecht, Phys. Rev. Letters 19, 1093 (1967); G. Bret and H. Weber, IEEE J. Quantum Electron. QE-4, 807 (1968); M. J. Colles, Opt. Commun. 1, 169 (1969); M. A. Bolshov, Yu. I. Golyaev, V. S. Dneprovskii, and I. I. Nurminskii, Zh. Eksperim. i Teor. Fiz. 57, 346 (1969) [Sov. Phys. JETP 30, 190 (1970)]; R. L. Carman, M. E. Mack, F. Shimizu, and N. Bloembergen, Phys. Rev. Letters 23, 1327 (1969); M. E. Mack, R. L. Carman, J. Reintjes, and N. Bloembergen, Appl. Phys. Letters 16, 209 (1970); M. J. Colles, G. E. Walrafen, and K. W. Wecht, Chem. Phys. Letters 4, 621 (1970).

[2]S. A. Akhmanov, Mat. Res. Bull. 4, 455 (1969); C. S. Wang, Phys. Rev. 182, 482 (1969); S. A. Akhmanov, A. P. Sakhorukov, and A. S. Chirkin, Zh. Eksperim. i Teor. Fiz. 55, 143 (1968) [Sov. Phys. JETP 28, 748 (1969)]; T. I. Kuznetsova, Zh. Eksperim. i Teor. Fiz. Pis'ma Redaktsiyu 10, 153 (1969) [Sov. Phys. JETP Letters 10, 98 (1969)]; N. M. Kroll and P. L. Kelley, Phys. Rev. A 4, 763 (1971).

[3]R. L. Carman, F. Shimizu, C. S. Wang, and N. Bloembergen, Phys. Rev. A 2, 60 (1970).

[4]R. L. Carman, M. E. Mack, F. Shimizu, and N. Bloembergen, Phys. Rev. Letters 23, 1327 (1969).

[5]H. Haken and M. Paunthier, IEEE J. Quantum Electron. QE-4, 454 (1968).

[6]M. E. Mack, R. L. Carman, J. Reintjes, and N. Bloembergen, Appl. Phys. Letters 16, 209 (1970).

[7]M. E. Mack, IEEE J. Quantum Electron. QE-4, 1015 (1968).

[8]Self-focusing in an externally focused beam has been observed and discussed by R. L. Carman, J. Reintjes, and M. E. Mack, in Proceedings of the IEEE International Quantum Electronics Conference, Kyoto, Japan, 1970 (unpublished).

[9]T. K. Gustafson (private communication).

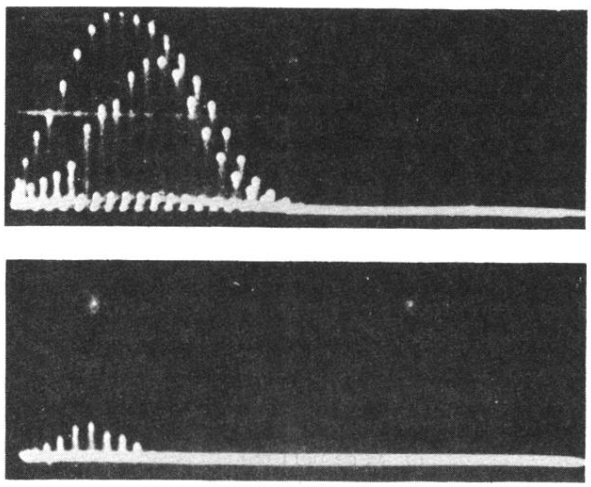

FIG. 2. Oscillograms of pulse trains demonstrating high Raman conversion: (a) interleafed incident and transmitted laser pulses; (b) generated Stokes-pulse train.

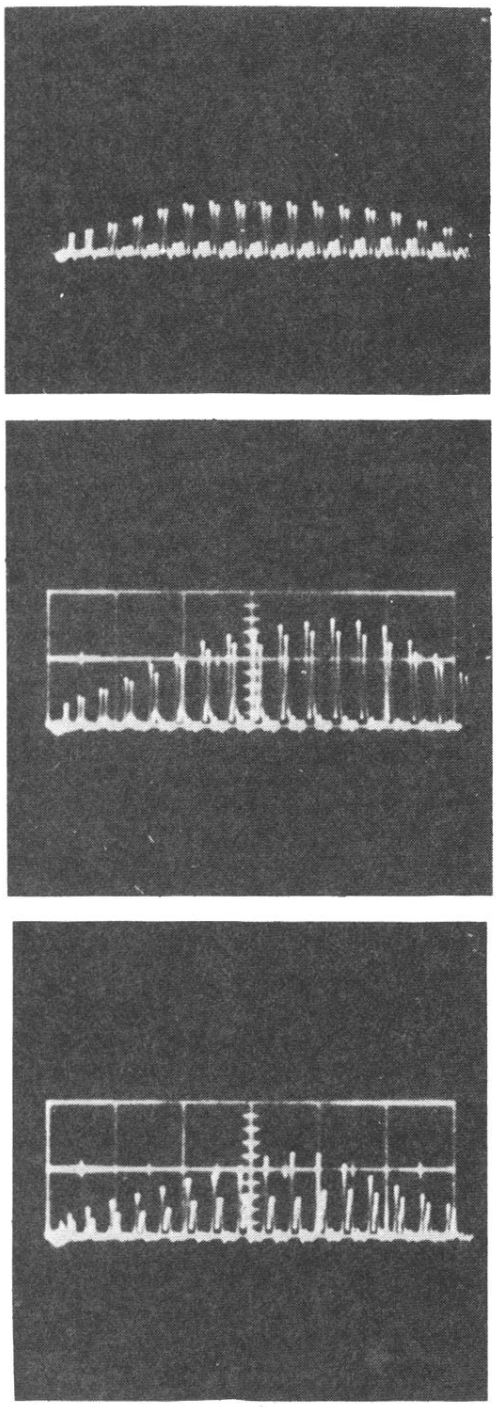

FIG. 3. Oscillograms of interleafed incidence and transmitted laser-pulse trains. (a) Typical oscillogram under conditions where the laser depletion was small enough to be acceptable; (b) marginal laser depletion; (c) example of unacceptably large laser depletion.

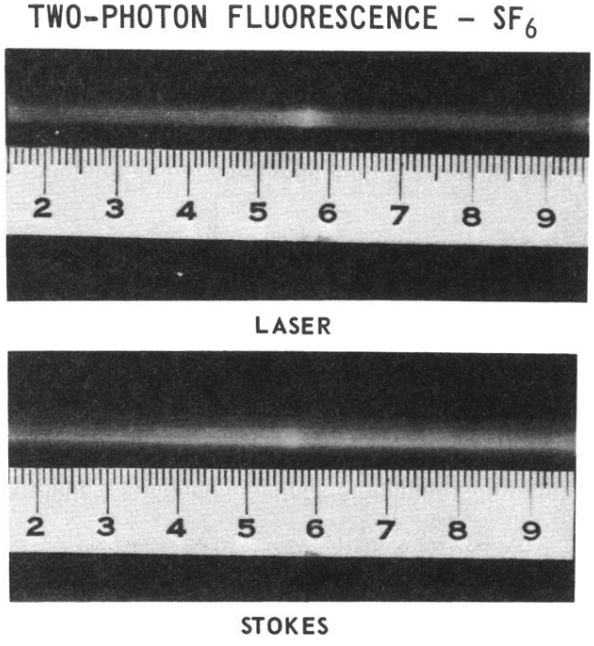

FIG. 4. Example of two-photon absorption fluorescence data under conditions of 2.5-psec-duration excitation, demonstrating shorter duration generated Stokes pulses.

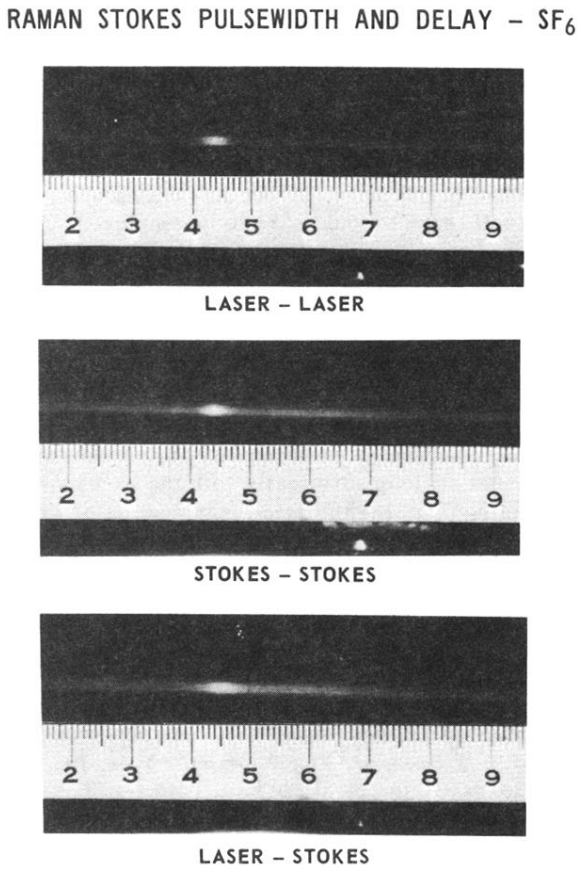

FIG. 6. Typical two-photon absorption fluorescence data taken using approximately a 15-psec-duration laser pulse. Note that the laser Stokes pattern is displaced, demonstrating a delay between the Stokes and Laser intensity maxima.